Available online at www.sciencedirect.com
ScienceDirect
Journal of Power Sources 162 (2006) 589–596
JOURNAL OF POWER SOURCES
www.elsevier.com/locate/jpowsour

High power-density single-chamber fuel cells operated on methane

Zongping Shao [1], Jennifer Mederos, William C. Chueh, Sossina.M. Haile *

Materials Science, Chemical Engineering, California Institute of Technology, Pasadena, CA 91125, United States

Received 26 May 2006; received in revised form 30 June 2006; accepted 3 July 2006
Available online 22 August 2006

Abstract

Single-chamber solid oxide fuel cells (SC-SOFCs) incorporating thin-film $Sm_{0.15}Ce_{0.85}O_{1.925}$ (SDC) as the electrolyte, thick Ni + SDC as the (supporting) anode and SDC + BSCF ($Ba_{0.5}Sr_{0.5}Co_{0.8}Fe_{0.2}O_{3-\delta}$) as the cathode were operated in a mixture of methane, oxygen and helium at furnace temperatures of 500–650 °C. Because of the exothermic nature of the oxidation reactions that occur at the anode, the cell temperature was as much as 150 °C greater than the furnace temperature. Overall, the open circuit voltage was only slightly sensitive to temperature and gas composition, varying from ∼0.70 to ∼0.78 V over the range of conditions explored. In contrast, the power density strongly increased with temperature and broadly peaked at a methane to oxygen ratio of ∼1:1. At a furnace temperature of 650 °C (cell temperature ∼790 °C), a peak power density of 760 mW cm^{-2} was attained using a mixed gas with methane, oxygen and helium flow rates of 87, 80 and 320 mL min^{-1} [STP], respectively. This level of power output is the highest reported in the literature for single chamber fuel cells and reflects the exceptionally high activity of the BSCF cathode for oxygen electro-reduction and its low activity for methane oxidation.

Keywords: Single chamber fuel cell; Methane; Ceria electrolyte

1. Introduction

The concept of the so-called single chamber fuel cell (SCFC) has been known in the literature for many years [1–3], but only recently have such fuel cells been demonstrated with competitive power densities [4–10]. In the single chamber configuration, the anode and cathode are exposed to the same reactant gas, a fuel–oxidant mixture [10]. Voltage across the cell is generated as a result of the differential catalytic activity (both chemical and electrochemical) of the anode and cathode towards the fuel–oxidant mixture. Typically, a lighter hydrocarbon (methane, propane, etc.) serves as the fuel while oxygen serves as the oxidant. The ideal anode should catalyze the partial oxidation of the hydrocarbon fuel to syngas ($CO + H_2$) as well as catalyze the electro-oxidation of these products, whereas the ideal cathode should be entirely inert towards the hydrocarbon fuel yet catalyze the electro-reduction of the oxygen gas.

In comparison to conventional dual-chamber solid-oxide fuel cells (SOFCs), single chamber SOFCs offer the advantages of quick start-up, simple stack design and gas management, and robustness against thermal cycling, all of which result from the seal-less operation. These advantages come at the expense of lower fuel efficiency, which results from incomplete fuel utilization and parasitic, non-electrochemical fuel oxidation (*i.e.* direct chemical oxidation). For portable and micropower applications, rapid start-up and high energy density are more important than the maximization of efficiency. Consequently, despite their limited fuel efficiency, single chamber SOFCs (SC-SOFCs) are attractive alternatives to batteries in the micropower arena.

In previous studies we reported the behavior of anode-supported thin-film ceria-based SCFCs operated on propane [6–8]. A maximum peak power density of 440 mW cm^{-2} was obtained at a cell temperature of ∼700 °C (furnace temperature of 500 °C) and a propane to oxygen ratio of 4:9 [8]. Higher temperature operation lowered the power output and this behavior was interpreted to result from propane oxidation at the cathode [7]. Compared to propane, methane is a relatively stable molecule. As a consequence, one can immediately anticipate that methane fueled SCFCs will require higher operational temperatures than those fueled by propane. High temperature conditions, in turn, can be beneficial if they increase cathode kinetics for oxygen electro-reduction without substantially lowering fuel cell voltage as a result of increased electronic conductivity in the

* Corresponding author. Tel.: +1 626 395 2958; fax: +1 626 395 8868.
E-mail address: smhaile@caltech.edu (Sossina.M. Haile).
[1] Present address: College of Chemistry and Chemical Engineering, Nanjing University of Technology, PR China.

0378-7753/$ – see front matter © 2006 Elsevier B.V. All rights reserved.
doi:10.1016/j.jpowsour.2006.07.003

ceria electrolyte or increased oxidation of the fuel at the cathode. If these conditions are met, operation on methane can be anticipated to lead to higher power densities than can be achieved from more reactive alkanes and this hypothesis is explored here. A selected set of the fuel cell polarization results described here have been reported elsewhere, as part of a computational study of single chamber fuel cell behavior [11]. In this work, we present a more extensive examination of the environmental parameters affecting fuel cell power output.

2. Fuel cell fabrication

In analogy to our earlier studies [6–8], the electrolyte and anode components of the fuel cell of the present investigation were comprised, respectively, of 15% samaria doped ceria (SDC) and of Ni + SDC (NiO:SDC = 60:40 wt. ratio) cermets. The cathode was composed of $Ba_{0.5}Sr_{0.5}Co_{0.8}Fe_{0.2}O_{3-\delta}$ (BSCF) + SDC (70:30 wt. ratio). The SDC powder was a mixture of commercial powder obtained from NexTech and in-house synthesized powder prepared by an EDTA-citrate sol–gel method [12]. The NiO powder was that obtained from Alfa Aesar (green, particle size < 35 μm) combined with that obtained from Aldrich (black, particle size < 10 μm). The BSCF powder was synthesized in-house, also by an EDTA-citrate method.

The fuel cells were fabricated by dual dry pressing of the anode-electrolyte bilayer followed by colloidal spray deposition of the cathode. Prior to application of the cathode, the anode-supported thin film electrolyte was sintered at 1350 °C for 5 h under air and then reduced at 600 °C for 2 h under diluted hydrogen to convert NiO in the anode to Ni. Subsequent to the cathode deposition, the entire tri-layer structure was sintered at 1000 °C for 8–12 h under inert atmosphere. The disk shaped fuel cells had a final diameter of 13.3 mm, anode porosity and thickness of ∼50% and ∼700 μm, respectively, electrolyte thickness of ∼20 μm and cathode thickness and effective area of 5–10 μm and 0.71 cm^2, respectively. Typical scanning electron microscopy (SEM) images of a fuel cell so prepared are presented in Fig. 1. The high degree of electrolyte densification obtained under these fabrication conditions is evident.

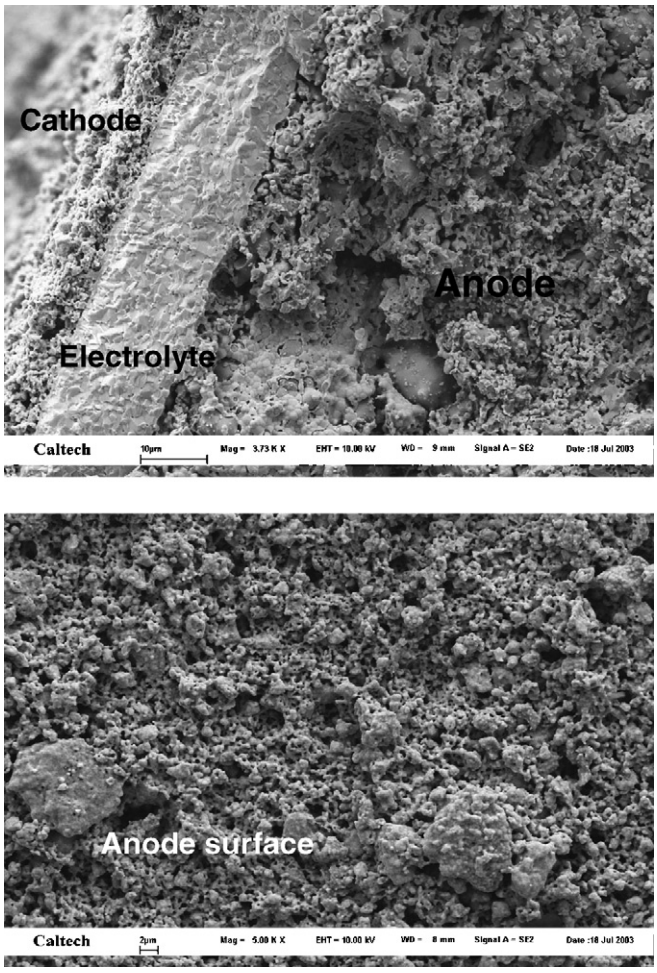

Fig. 1. Scanning electron microscopy images of typical fuel cell structures. Upper shows MEA (membrane electrode assembly) in cross-section and lower shows the porous surface of the anode in plan view.

3. Characterization

Chemical and electrochemical characteristics were evaluated using a conventional flow-through, tubular, quartz reactor (inner diameter = 15.9 mm) oriented vertically and with the flow directed downwards [7] (Fig. 2). In particular, the chemical activity of the cathode material, BSCF, for oxidation of propane, ethane and methane was examined as follows. A mixture of the reactant gases was passed over BSCF diluted with quartz powder and the composition of the product gases measured. The BSCF powder used for these measurements was prepared as described above for fuel cell fabrication. The specific surface area was determined by the BET method using a Micromeritics Gemini 2365 surface area analyzer, with N_2 as the adsorbate gas and found to be ∼0.25 $m^2\ g^{-1}$. Sample quantities were 0.2–0.3 g BSCF, mixed with 1.2 g quartz powder. (The quartz powder was tested for catalytic inactivity prior to data collection.) The reactor feed (fuel, oxygen and helium diluent) was maintained at a constant total flow rate of 130 mL min^{-1} (at STP, standard temperature and pressure, where STP is implied hereafter and not stated) and reactant flows were individually measured by mass flow meters before mixing. The fuel and oxygen reactants were highly diluted by helium in order to minimize the total volumetric change upon reaction. At the beginning of each measurement, the BSCF sample was pre-treated for 5 h under a stoichiometric fuel:oxygen ratio, at the highest test temperature, in order to stabilize the catalytic activity. Reaction products were characterized in an in-line Varian CP-4900 Micro-GC, capable of detecting, in addition to hydrocarbons, CO, CO_2 and O_2. Hydrocarbon conversion at the outlet was determined by balancing the carbon in the product stream.

For the measurement of electrochemical properties, silver wire, net and paste were applied as current collectors to either side of the complete fuel cells; platinum was not used for this purpose in order to avoid the catalysis that would be expected to occur over this metal. Polarization curves were obtained using a 4-probe technique to eliminate the effect of the wire resistances. Measurements were performed at furnace temperatures of 500–650 °C with an inlet gas composed of

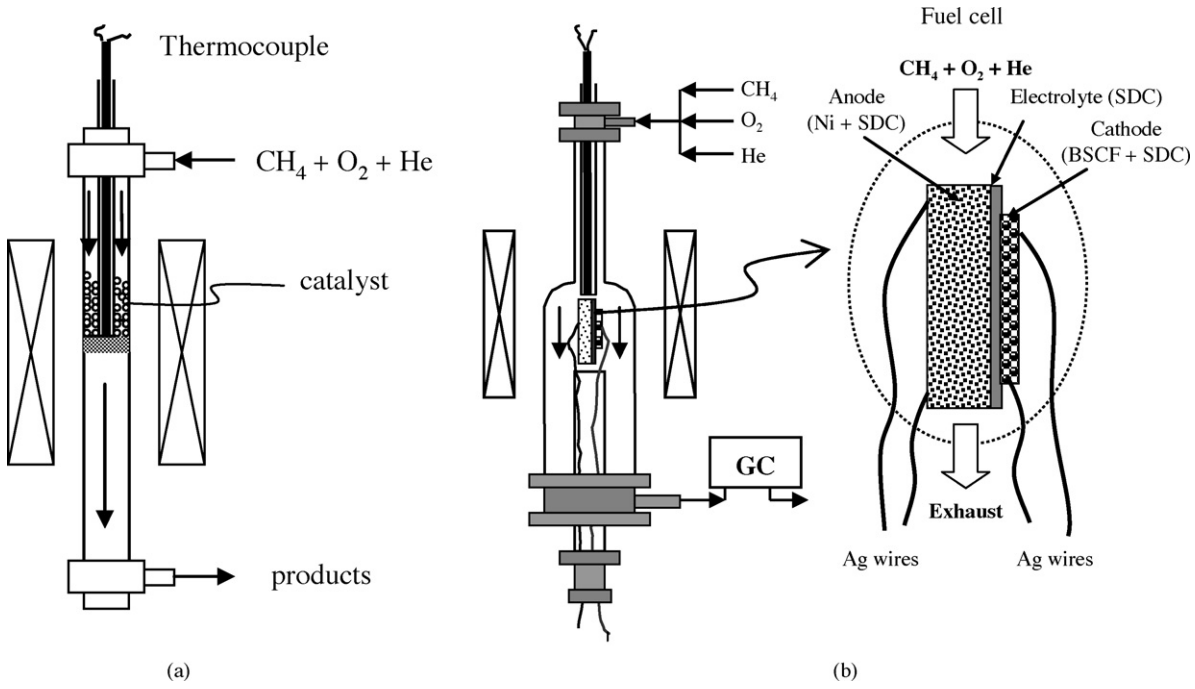

Fig. 2. Flow-through reactor used for the evaluation of cathode catalytic activity, as configured in (a) and of fuel cell electrochemical properties, as configured in (b).

methane + oxygen + helium supplied at rates of 87, 70–90 and 280–360 mL min^{-1}, respectively. The O_2:He volumetric ratio was maintained at 1:4 in order to simulate the oxygen content of air. Helium rather than N_2 was used to facilitate analysis of the off-gas composition; the micro GC signal of N_2 overlaps with that of O_2 at high concentrations. With this set of gas flow rates, the O_2/CH_4 ratio was varied from 0.80 to 1.03, corresponding to compositions that were 2.49–1.93 times rich in methane relative to the stoichiometric ratio for complete oxidation. The polarization data were collected upon cooling from the maximum furnace set temperature of 650 °C, in 25–50 °C increments. The fuel cell was raised to this initial temperature under helium at a heating rate of 20 °C min^{-1} and held there until thermal equilibrium was attained. At each temperature, the gas composition was stepped through the entire range examined before lowering the temperature to next value. Following each change in gas composition or temperature, the fuel cell was equilibrated for about a 5 min period prior to polarization data collection.

It is now well established that chemical (in addition to electrochemical) oxidation at the anode of SC-SOFCs, Eqs. (1) and (2) [13], can lead to a substantial temperature rise [14], which, in turn, impacts fuel cell electrical behavior.

$$CH_4(g) + 1/2O_2(g) = CO(g) + 2H_2(g),\ \Delta H_{650^\circ c} = -23.45\ kJ\ mol^{-1} \quad (1)$$

$$CH_4(g) + 2O_2(g) = CO_2(g) + 2H_2O(g),\ \Delta H_{650^\circ c} = -800.75\ kJ\ mol^{-1} \quad (2)$$

In order to evaluate the significance of this effect, the temperature rise at the anode of complete fuel cell MEA's was measured under open circuit conditions. The gas compositions utilized were similar to those employed for fuel cell polarization measurements. Specifically, the methane flow rate was fixed at 87 mL min^{-1}, the O_2/He ratio was fixed at 0.25 (again, to simulate air) and the oxygen flow rate was varied from 50 to 120 mL min^{-1} for an O_2/CH_4 ratio that varied from 0.6 to 1.4. Measurements were performed for furnace set temperatures ranging from 585 to 660 °C. A K-type thermocouple (protected by a thin wall quartz tube) was physically contacted to the center of the fuel cell anode surface. In principle, catalytic oxidation at the cathode could also contribute to the temperature rise, however, because of the much larger volume of the anode (700 μm in thickness as compared to only 5–10 μm for the cathode or 20 μm for the electrolyte), this component dominates the temperature response and temperature measurements directly at the anode are most relevant. Both the rate of temperature change in response to a change in environmental conditions and the thermal stability under fixed conditions were examined.

4. Results and discussion

4.1. Hydrocarbon oxidation over BSCF

Selected catalytic activity results are presented in Fig. 3 for oxygen to fuel ratios that are ∼2.5× that of stoichiometric. While comprehensive results and analysis of alkane oxidation over BSCF will be reported elsewhere, it is immediately apparent that methane oxidation over this perovskite indeed requires higher temperatures than does either propane or ethane oxidation, consistent with the relative stabilities of these three molecules. Light-off occurs at ∼450, 475 and 600 °C, respectively for propane, ethane and methane, whereas the conversion rates at 590 °C are 1.9, 1.3 and 0.17 mmol s^{-1} m^2, respectively (Fig. 3a). These rates are reported relative to the total surface area of BSCF placed in the reactor. A significant feature of catalysis

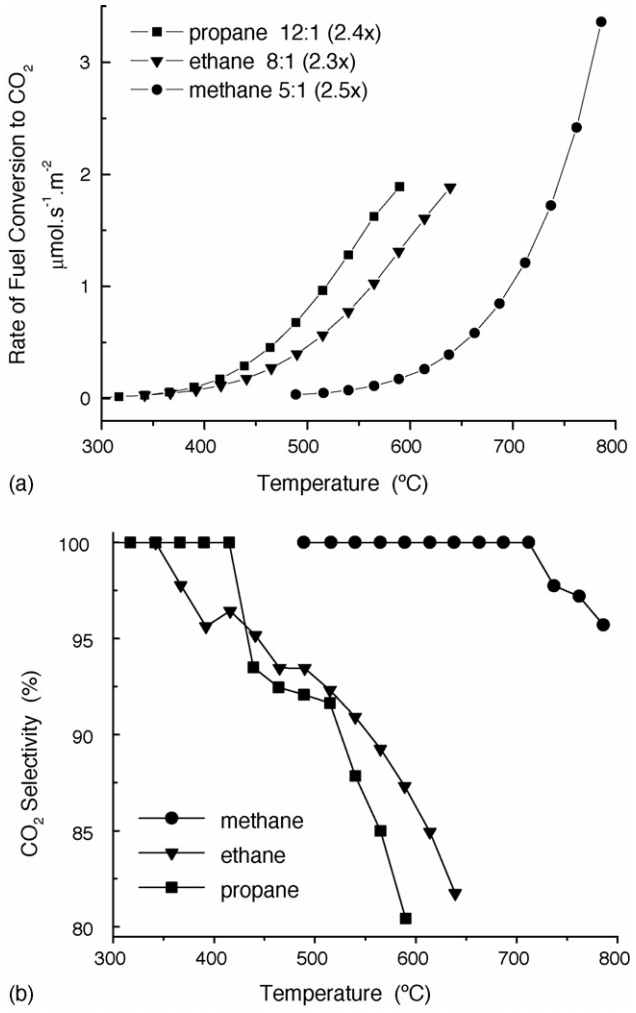

Fig. 3. Catalytic activity of $Ba_{0.5}Sr_{0.5}Co_{0.8}Fe_{0.2}O_{3-\delta}$ (BSCF) for the combustion of methane, ethane and propane at 2.3–2.5 times stoichiometric (as indicated). Ratios in legend are oxygen:fuel flow rates in mL min^{-1} (total flow rate = 130 mL min^{-1}, with helium providing balance of flow). (a) Rate of fuel conversion normalized to catalyst surface area and (b) percent selectivity for CO_2 (percent of carbon in reaction products present as CO_2).

over BSCF is that the primary carbon-bearing oxidation product is CO_2. This is particularly true in the case of methane, where essentially 100% of the reacted carbon appears in the form of CO_2 up to temperatures of 700 °C, dropping only slightly to ~95% at 800 °C (Fig. 3b). Thus, BSCF is inactive as a methane partial oxidation catalyst and only slightly active as a methane total oxidation catalyst. As a consequence, the hydrocarbon fuel passes by the cathode unreacted or a slight portion interacts such that it is completely oxidized. These features are useful for single chamber operation. The by-product CO_2 acts as a diluent at the cathode, but has much less effect on the oxygen chemical potential than the partial oxidation products CO and H_2. In the case of ethane and propane, a small portion of the carbon is converted to products such as C_3H_6 (propane < 2% of the entering carbon at the highest measurement temperature of 590 °C) and C_2H_4 (ethane < 4% of the entering carbon at the highest measurement temperature of 640 °C). Again, however, the bulk of the reacted carbon exists in the form of CO_2, with the CO_2 selectivity being greater than 80% for all measurement conditions. In all cases, the concentration of CO in the product stream is negligible, at most, just above the detection limit (0.07%) at the highest measurement temperatures for ethane and propane, whereas it is undetectable for methane.

4.2. Fuel cell polarization characteristics

A selection of the power densities and polarization (I–V) curves obtained from these fuel cells at several temperatures and at fixed gas compositions are presented in Figs. 4 and 5. The data in Fig. 4 were obtained for a gas composition of 87 mL min^{-1} CH_4 + 75 mL min^{-1} O_2 + 300 mL min^{-1} He, whereas the gas composition for the data in Fig. 5 was 87 mL min^{-1} CH_4 + 90 mL min^{-1} O_2 + 360 mL min^{-1} He, representing the most fuel rich and fuel lean conditions explored, respectively. Both the furnace set temperature (T_f) and the estimated cell temperature (T_c) are reported in the figures. The cell temperatures are those obtained from separate measurements

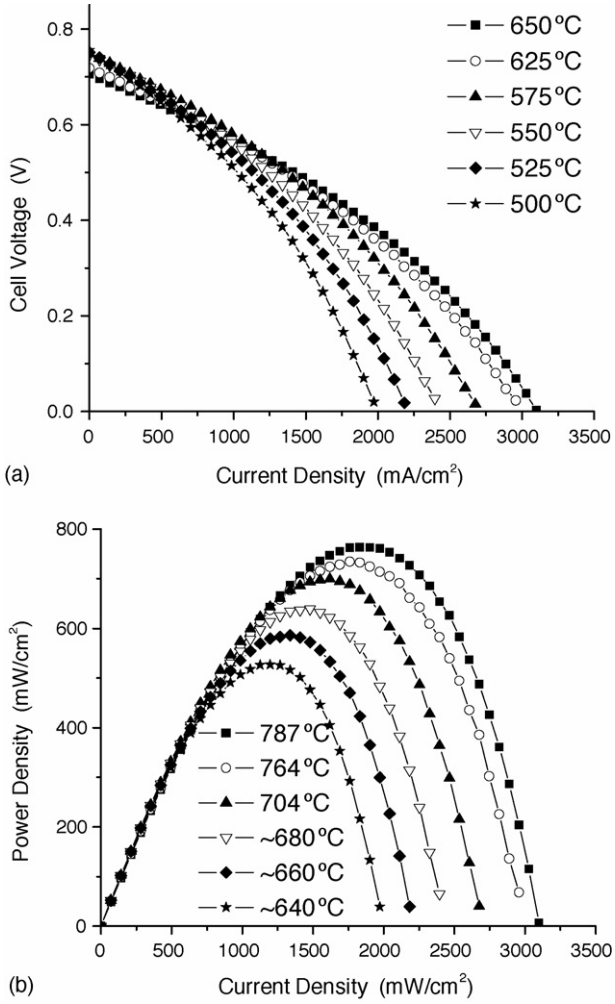

Fig. 4. (a) Polarization and (b) power density curves obtained under a gas composition of 87 mL min^{-1} CH_4 + 75 mL min^{-1} O_2 + 300 mL min^{-1} He, the most fuel rich conditions examined. Legend in (a) indicates both the furnace set temperature (T_f) and the approximate cell temperature (T_c) as T_f/T_c; see text for discussion of cell temperature.

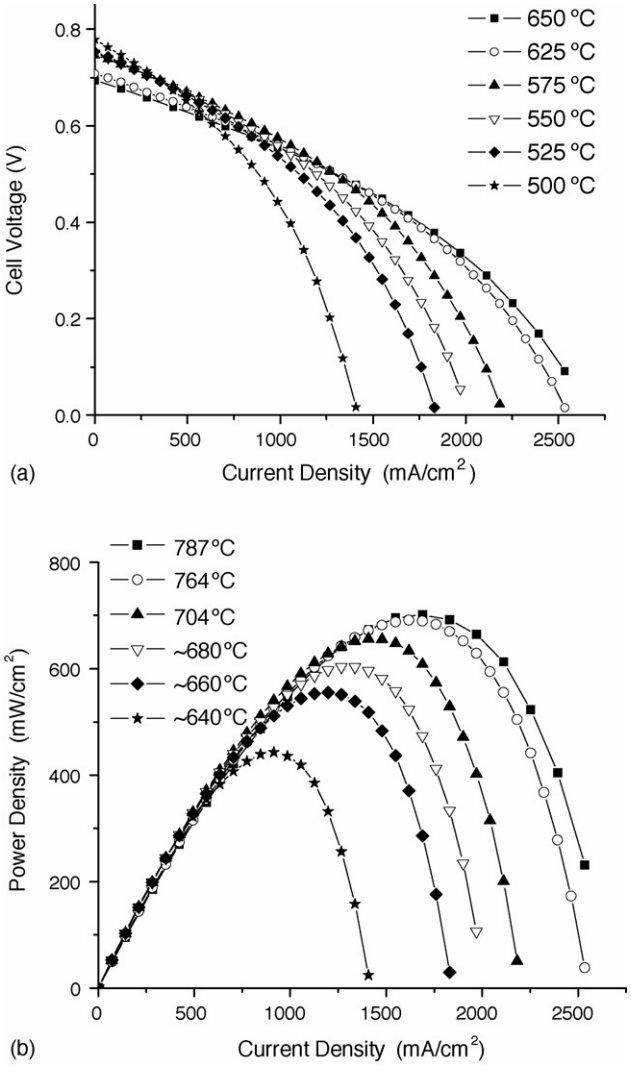

Fig. 5. (a) Polarization and (b) power density curves obtained under a gas composition of 87 mL min^{-1} CH_4 + 90 mL min^{-1} O_2 + 360 mL min^{-1} He, the most fuel lean conditions examined. Legend in (a) indicates both the furnace set temperature (T_f) and the approximate cell temperature (T_c) as T_f/T_c; see text for discussion of cell temperature.

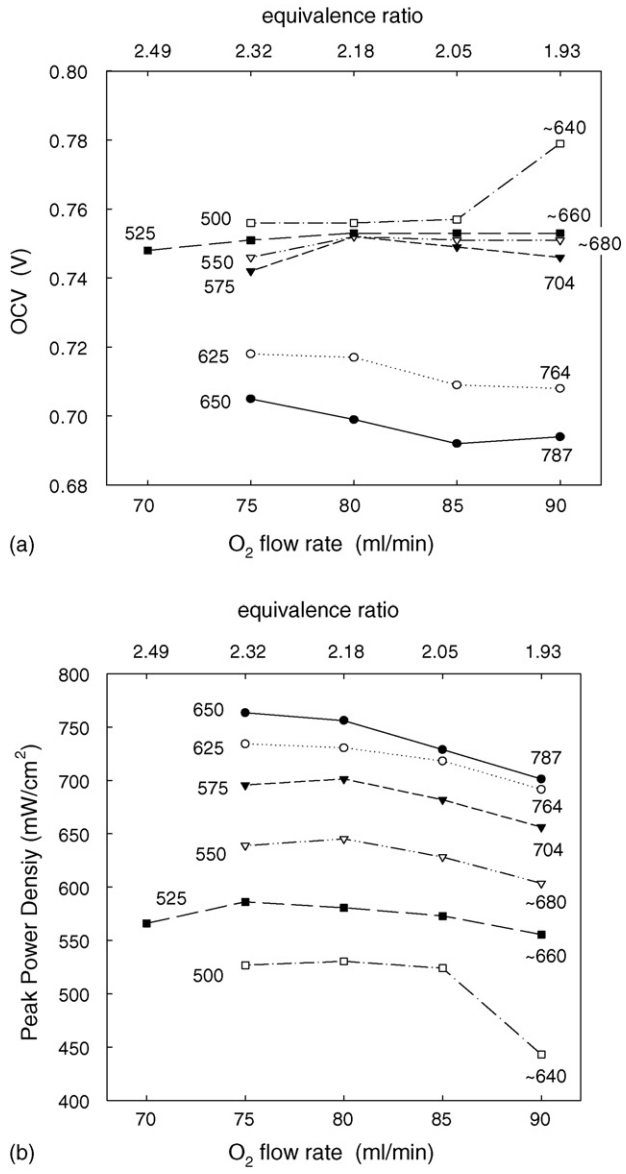

Fig. 6. A summary of the (a) open circuit voltages (OCVs) and (b) peak power densities measured in single chamber fuel cells at the temperatures indicated (left, furnace temperature and right, cell temperature) as functions of oxygen flow rate for a fixed methane flow rate of 87 mL min^{-1} and a helium flow rate four times that of the oxygen flow rate.

under open circuit conditions (discussed further below). At the lowest furnace temperature examined, 500 °C, it was found that after several hours the power output fell to zero. The results presented in Figs. 4 and 5 reflect polarization measurements that were completed within 1 h of lowering the furnace temperature from 550 °C. A summary of the open circuit voltages (OCVs) and peak power densities obtained from the full range of measurement conditions examined is provided in Fig. 6, where the data are shown as functions of oxygen flow rate for the fixed methane flow rate of 87 mL min^{-1}.

Overall, the specific power densities resulting from these fuel cells were extremely high and moderately sensitive to the environmental conditions of temperature and gas phase composition. The highest power output was obtained at the highest temperature (T_f = 650 °C) and most fuel rich gas composition examined (CH_4:O_2 = 87:75). Under these conditions, the OCV, the limiting current and peak power density were 0.71 V, 3.1 A cm^{-2} and 760 mW cm^{-2}, respectively. This power density is the highest reported to date in the literature for a single chamber fuel cell and is, in fact, comparable to the values obtained from direct methane fueled dual chamber SOFCs [15,16]. We attribute this exceptional power output to the combination of high oxygen reduction activity and low methane oxidation activity of the BSCF cathode combined with the thinness of the ceria electrolyte employed here. The power densities are furthermore higher than achieved using propane as the fuel [8] with essentially identical fuel cells because of the greater chemical stability of methane. As indicated in Fig. 3, this feature enables fuel cell operation at higher temperatures than with propane, enhancing oxygen electro-reduction at the cathode and increasing ionic conductivity through the electrolyte.

Within the range of parameters explored, the peak power density was more sensitive to furnace temperature, exhibiting a monotonic increase with increasing temperature, than to gas composition. For a given gas composition, the peak power density at a furnace temperature of 650 °C was about 250 mW cm^{-2} higher than at 500 °C. In contrast, the power output displayed an apparent broad peak at a methane to oxygen ratio of about 1:1, with the peak position shifting to more fuel rich compositions with increasing temperature, possibly to higher than even 1.16:1 which represents the most fuel rich conditions examined. For complete oxidation of the fuel (to yield CO_2 and H_2O) a methane to oxygen ratio of 0.5:1 is required, whereas the ideal ratio for partial oxidation is 2:1. Thus, it appears that the optimal value for single chamber fuel cell operation lies between these two extremes. This observation agrees with the results reported by Hibino, who also found an optimal methane to oxygen ratio of ~1:1 for maximal power output [9]. Such a methane to oxygen ratio also roughly coincides with the reactant gas composition that yields the highest concentration of partial oxidation products CO and H_2 under equilibrium conditions at these temperatures [17].

In contrast to the peak power density, the open circuit voltage decreased slightly with increasing temperature, dropping by about 50 mV for the most fuel rich conditions over the (furnace) temperature range of 500–650 °C. Furthermore, under all conditions the voltages are low when compared to conventional, zirconia-based dual-chamber fuel cells (typically ~1 V depending on the exact anode and cathode gas compositions). Several factors give rise to the low OCVs in the present cells: insufficient chemical activity of the anode catalyst, chemical activity of the cathode catalyst for fuel combustion, electronic conductivity of the ceria electrolyte, insufficient electrochemical activity of the electrodes, and gas phase transport of the partial oxidation products H_2 and CO from the anode to the cathode side of the fuel cell. An approximate evaluation of the contribution of a selection of these factors is presented in Fig. 7. Here, the measured OCV is shown as a function of temperature for the most fuel rich conditions and compared to (1) the OCV expected for an ideal single chamber fuel cell with a purely ionically conducting electrolyte and ideally active electrodes, (2) the OCV expected for a single chamber fuel cell in which the electronic conductivity is that as measured for SDC15 [18], but retaining ideally active electrodes and (3) the OCV expected for the SCFC as in case (2) but also accounting for non-ideal electrochemical activity of the electrodes. For this evaluation the oxygen partial pressure at the cathode is taken to be identical to that of the inlet gas, whereas that at the anode is taken to be the value which results from chemical equilibration of the inlet gases (calculated using the software package HSC [17]). The influence of electronic conductivity through the electrolyte was calculated according to the method of Riess [19] and the influence of the insufficient electrochemical activity of the electrodes was estimated from preliminary EMF (electromotive force) measurements of the BSCF|SDC15|Ni + SDC15 system under dual chamber conditions. Those data indicate the voltage drop across the electrodes to amount to ~120 mV, independent of temperature [20].

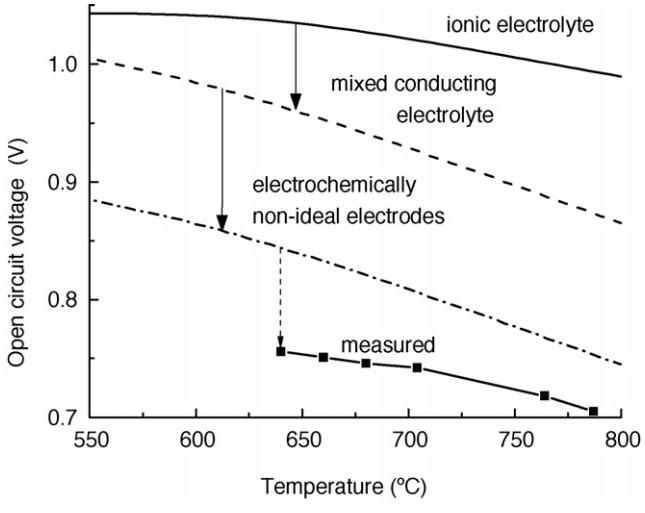

Fig. 7. Comparison between measured and calculated open circuit voltages as functions of temperature for a ceria based single chamber fuel cell; see text for discussion of calculation methodologies.

The data in Fig. 7 demonstrate that the difference between the measured and calculated OCV when the mixed conducting characteristics of the ceria electrolyte are fully accounted for is greatest at low temperatures. Thus, factors such as gas phase transport of the partial oxidation products from anode to cathode side of the fuel cell and catalytic combustion of the methane at the cathode, which become more significant at higher temperatures, are unlikely to be key limiters to the fuel cell OCV and thereby power output. Instead, it appears that the anode, presumably being less effective at producing the equilibrium gas composition at low temperature than at high temperature, is responsible for the observed behavior. Stated alternatively, the difference between the equilibrium and actual gas concentration at the anode is greatest at low temperature. At high temperatures, the electronic conductivity of the electrolyte is apparently the largest factor responsible for the low OCV. This result is consistent with the observation of Hibino et al. [21] that yttria stabilized zirconia (YSZ) and LSGM ($La_{0.9}Sr_{0.1}Ga_{0.8}Mg_{0.2}O_3$) electrolyte fuel cells exhibit open circuit voltages that are more than 100 mV larger than those from ceria electrolyte fuel cells when operated in single chamber mode on methane at a nominal (furnace) temperature of 700 °C.

In terms of fuel cell power output, one requires not only that the oxygen partial pressure be low at the anode so as to generate a high OCV, but also that the concentration of partial oxidation products, CO and H_2, be high, as it these species which can be electrochemically consumed. At low temperatures, in addition to an overall low activity of the Ni anode for CH_4 and O_2 conversion (as indicated by the low OCV), the anode exhibits poor selectivity for the production of CO and H_2 as opposed to CO_2 and H_2O [21]. As a consequence, the anode characteristics limit the cell voltage not only under open circuit conditions, but also under fuel cell operational conditions and thus limit the power output. Developing an anode catalyst that is both more active for methane and oxygen conversion and more selective for CO and H_2 generation is essential for improving the fuel cell performance at low temperatures. At high temperatures, the data suggest that the electronic conductivity of the ceria electrolyte is

the key-limiting factor for power output. It must be emphasized, however, that simply replacing the ceria electrolyte with yttria stabilized zirconia (YSZ) within the materials set utilized here is not possible because of the reactivity of YSZ with the BSCF cathode [22]. On the other hand, there are no known SOFC cathodes that match either the electrochemical activity of BSCF for oxygen electro-reduction or its chemical inactivity for alkane combustion [8] and identifying a viable alternative will likely be a tremendous challenge.

4.3. Thermal behavior

The thermal response of the complete fuel cell MEAs at selected furnace temperatures is presented in Fig. 8. The data illustrate the rate of fuel cell temperature change in response to a change in environmental conditions, as well as the significant dependence on furnace set-temperature of the steady-state temperature difference between the fuel cell and furnace temperatures. For this set of measurements, the cell was equilibrated with the furnace under flowing helium at each temperature prior to the introduction of the reactant gas stream. The cell temperature was recorded as a function of time (under OCV conditions) upon commencing the reactant gas flow, comprising in this example 87 mL min^{-1} CH_4 + 80 mL min^{-1} O_2 + 320 mL min^{-1} He.

At almost all furnace set temperatures (T_f) the fuel cell temperature (T_c) reached a steady state value within 3 min (Fig. 8a). The sole exception occurred for a furnace temperature of 585 °C, which required longer than 10 min for the temperature to stabilize. Under steady state conditions (Fig. 8b), the difference between T_f and T_c was only 5 °C at a furnace temperature of 462 °C, but rose with increasing furnace temperature, as would be expected. The most rapid increase occurs between furnace temperatures of 561 and 585 °C; at T_f = 585 °C the difference between the cell and furnace temperatures is 152 °C, corresponding to a cell temperature of 737 °C. This behavior, which indicates catalytic ignition of the oxidation reaction at a cell temperature somewhere between 619 and 737 °C, is consistent with the conclusion drawn based on the analysis of the OCV results that nickel is relatively inactive for oxygen chemical conversion at low temperatures.

An important characteristic of these cells is that equilibration times are much longer if the cell is not first thermally equilibrated with the furnace via a helium purge. This is evidenced from the data in Fig. 9, where the change in cell temperature response to a change in furnace temperature (lowered from 585 to 561 °C) is shown for a fuel cell in which the reactant gas flow has not been interrupted with helium. The reactant gas flow is identical to that of the helium purge experiments (87 mL min^{-1} CH_4 + 80 mL min^{-1} O_2 + 320 mL min^{-1} He). Within the first 25 min after the temperature change, the cell temperature drops from about 740 to 710 °C and then remains at this value for another 2 h. Only after a total equilibration time of over 2.5 h, the temperature drops to the final steady state value of 619 °C, which coincides with that measured from experiments utiliz-

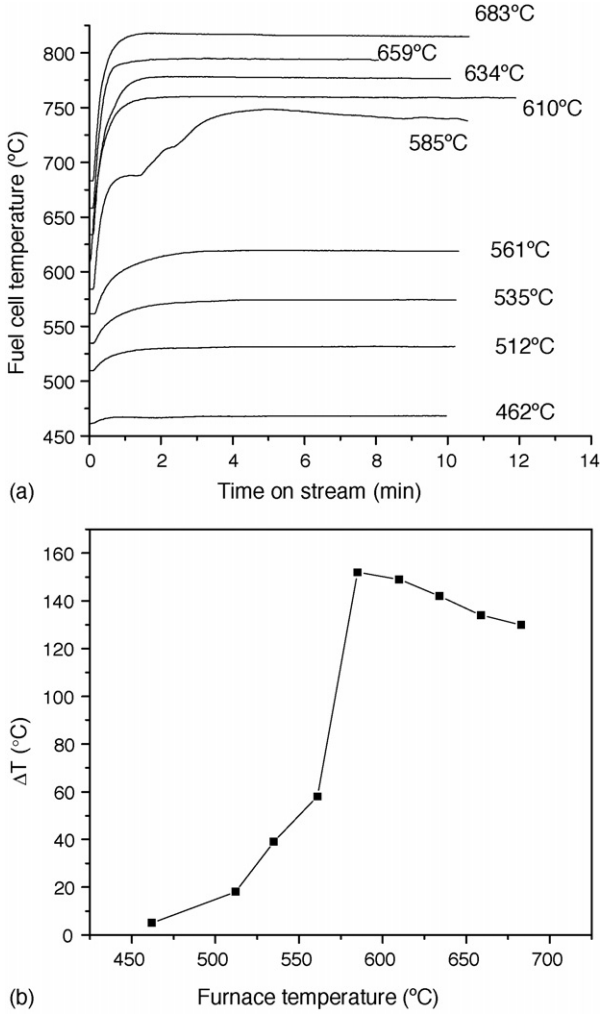

Fig. 8. Fuel cell temperature (a) as a function of time upon introduction of the reactant flow gas {CH_4: 87 mL min^{-1}[STP] + O_2: 80 mL min^{-1}[STP] + He: 320 mL min^{-1}[STP]} with furnace temperature as indicated and (b) as a function of furnace temperature after equilibration.

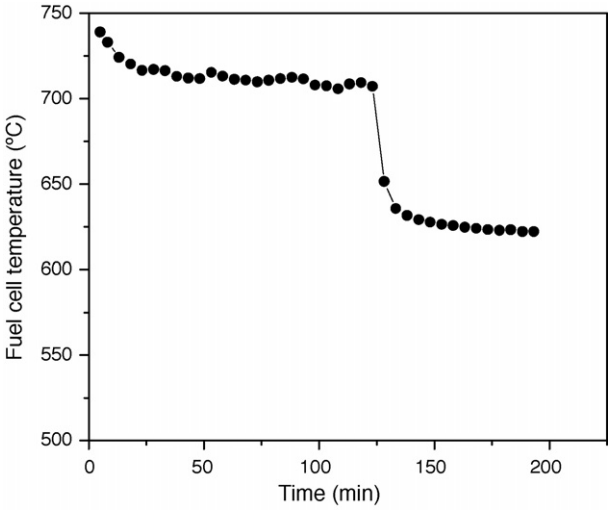

Fig. 9. Fuel cell temperature as a function of time upon lowering the furnace temperature from 585 °C (T_c = 707 °C) to 561 °C while maintaining the reactant gas flow of 87 mL min^{-1} CH_4 + 80 mL min^{-1} + O_2 + 320 mL min^{-1} He.

ing a helium purge. This behavior explains why it is possible to obtain measurable fuel cell power output for a furnace set temperature of 500 °C that subsequently falls to zero with time. The cell temperature during power output likely corresponds to a quasi-equilibrated value that could well be as high as 640 °C (the value reported in Figs. 4 and 5), rather than the fully equilibrated value of 517 °C. The result further emphasizes the importance of incorporating higher activity anode catalysts for enhancing single chamber fuel cell power output.

5. Conclusions

The performance of Ni + SDC|SDC|BSCF + SDC anode-supported thin film electrolyte SCFCs operated on methane has been presented. Because of the exothermic nature of the oxidation reactions that occur at the anode, the cell temperature was as much as 150 °C greater than the furnace temperature. The catalytic oxidation reactions furthermore can lead to excessively long thermal equilibration times, particularly on cooling. At a furnace temperature of 650 °C (cell temperature ∼790 °C), a peak power density of 760 mW cm^{-2} was attained using a mixed gas with methane, oxygen and helium flow rates of 87, 80 and 320 mL min^{-1}, respectively. This level of power output is the highest reported in the literature for single chamber fuel cells and reflects the exceptionally high activity of the BSCF cathode for oxygen electro-reduction and its low activity for methane oxidation. The power output of these cells is limited at low temperatures by the poor catalytic activity of Ni for methane partial oxidation and at high temperatures by the electronic conductivity of the ceria electrolyte. The open circuit voltage decreases only slightly with increasing temperature, whereas the power density is a strongly increasing function of temperature. At high temperature, the benefits of increased catalytic activity at the anode, increased ion transport rates and increased electrochemical activity at both anodes apparently outweigh the penalties of increased electronic conductivity through the electrolyte and increased parasitic combustion at the cathode. This thermal behavior contrasts that of propane fueled SCFCs in which high temperature operation is limited by parasitic catalytic combustion of the fuel at the cathode. The overall cell behavior is less sensitive to gas composition than temperature. The peak power density broadly peaks at a methane to oxygen ratio of 1:1, which loosely coincides with the composition which yields the highest concentration of partial oxidation products under equilibrium conditions at these high temperatures.

Acknowledgements

The authors gratefully acknowledge Dr. Shaomin Liu (formerly of Caltech) for providing a portion of the BSCF powder used in this work, Dr. Ma Chi for assistance with acquisition of scanning electron microscopy images and Prof. Janet Hering for providing access to surface area analysis instrumentation. This work was funded by the Defense Advanced Research Projects Agency, Microsystems Technology Office. Additional support was provided by the National Science Foundation through the Caltech Center for the Science and Engineering of Materials.

References

[1] W. van Gool, The possible use of surface migration in fuel cells and heterogeneous catalysis, Philips Res. Rep. 20 (1965) 81.
[2] C.K. Dyer, A novel thin-film electrochemical device for energy-conversion, Nature 343 (1990) 547.
[3] T. Hibino, H. Iwahara, Simplification of solid oxide fuel-cell system using partial oxidation of methane, Chem. Lett. (1993) 1131.
[4] X. Jacques-Bedard, T.W. Napporn, R. Roberge, M. Meunier, Performance and ageing of an anode-supported sofc operated in single-chamber conditions, J. Power Sources 153 (2006) 108.
[5] T. Suzuki, P. Jasinski, V. Petrovsky, H.U. Anderson, F. Dogan, Performance of a porous electrolyte in single-chamber SOFCs, J. Electrochem. Soc. 152 (2005) A527–A531.
[6] Z.P. Shao, S.M. Haile, J. Ahn, P.D. Ronney, Z.L. Zhan, S.A. Barnett, A thermally self-sustained micro solid-oxide fuel-cell stack with high power density, Nature 435 (2005) 795.
[7] Z.P. Shao, C. Kwak, S.M. Haile, Anode-supported thin-film fuel cells operated in a single chamber configuration, Solid State Ionics 175 (2004) 39.
[8] Z.P. Shao, S.M. Haile, A high-performance cathode for the next generation of solid-oxide fuel cells, Nature 431 (2004) 170.
[9] T. Hibino, A. Hashimoto, M. Yano, M. Suzuki, S. Yoshida, M. Sano, High performance anodes for SOFCS operating in methane-air mixture at reduced temperatures, J. Electrochem. Soc. 149 (2002) A133–A136.
[10] T. Hibino, A. Hashimoto, T. Inoue, J. Tokuno, S. Yoshida, M. Sano, A low-operating-temperature solid oxide fuel cell in hydrocarbon-air mixtures, Science 288 (2000) 2031.
[11] Y. Hao, Z. Shao, J. Mederos, W. Lai, D.G. Goodwin, S.M. Haile, Recent advances in single-chamber fuel-cells: experiment and modeling, Solid State Ionics, in press, doi:10.1016/j.ssi.2006.05.0008.
[12] Z.P. Shao, W.S. Yang, Y. Cong, H. Dong, J.H. Tong, G.X. Xiong, Investigation of the permeation behavior and stability of a $Ba_{0.5}Sr_{0.5}Co_{0.8}Fe_{0.2}O_{3-\delta}$ oxygen membrane, J. Membr. Sci. 172 (2000) 177.
[13] NIST-JANAF, Thermochemical Tables, fourth ed., in: M.W. Chase (Ed.), Journal of Physical and Chemical Reference Data. Monograph No. 9, Amercian Chemical Society and American Institute of Physics, Washington DC.
[14] T. Hibino, A. Hashimoto, T. Inoue, J. Tokuno, S. Yoshida, M. Sano, A Solid oxide fuel cell using an exothermic reaction as the heat source, J. Electrochem. Soc. 148 (2001) A544–A549.
[15] J.A. Liu, S.A. Barnett, Operation of anode-supported solid oxide fuel cells on methane and natural gas, Solid State Ionics 158 (2003) 11.
[16] C.H. Wang, W.L. Worrell, S. Park, J.M. Vohs, R.J. Gorte, Fabrication and performance of thin-film YSZ solid oxide fuel cells, J. Electrochem. Soc. 148 (2001) A864–A868.
[17] Outokumpu Research Oy *HSC Chemistry for Windows Version 5.1* Finland, 2002.
[18] W. Lai, S.M. Haile, Impedance spectroscopy as a tool for chemical and electrochemical analysis of mixed conductors: a case study of ceria, J. Am. Ceram. Soc. 88 (2005) 2979.
[19] I. Riess, Theoretical treatment of the transport-equations for electrons and ions in a mixed conductor, J. Electrochem. Soc. 128 (1981) 2077.
[20] W. Lai, S.M. Haile, unpublished results.
[21] T. Hibino, A. Hashimoto, T. Inoue, J. Tokuno, S. Yoshida, M. Sano, Single-chamber solid oxide fuel cells at intermediate temperatures with various hydrocarbon-air mixtures, J. Electrochem. Soc. 147 (2000) 2888.
[22] J. Ho, S.M. Haile, unpublished results.